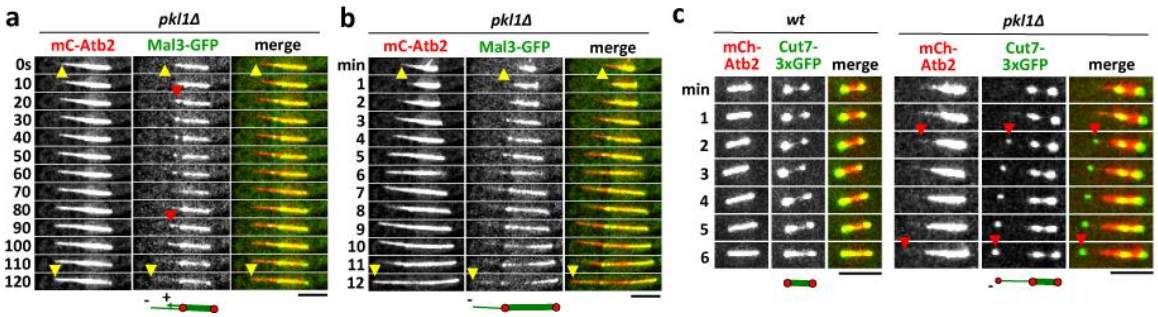

Supplementary Figure 1. Long MT protrusions are likely minus-ended MTs.

a) High-temporal resolution (10s interval) time-lapse images of a mitotic spindle of a *pkl1Δ* cell expressing mCherry-Atb2 and Mal3-GFP. Mal3-GFP is present all along the spindle. Distinct dot of Mal3-GFP tracks the short growing MT (red arrow head, time 20-60s), and disappears when the MT depolymerizes (time 70s). In contrast, the long MT has no Mal3-GFP at its tip (yellow arrow head). This long MT is stable and does not depolymerize. Note that the MT protrusion can contain more than one individual MT, with both Mal3-GFP labeling and no labeling. Scale bar, 5μm.

b) Low-temporal resolution (1min interval) time-lapse images of a mitotic spindle of a *pkl1Δ* cell expressing mCherry-Atb2 and Mal3-GFP. The long MT protrusion (yellow arrow head) persisted for 12min. This relatively stability is indicative of MT minus ends. Scale bar, 5μm.

c) Time-lapse images of *wt* and *pkl1Δ* mitotic cells expressing mCherry-Atb2 and Cut7-3xGFP (kinesin-5 cut7 can move toward to MT minus end [6]). In the *wt* cell, Cut7-3xGFP localizes to the spindle, and prominently at the spindle poles. In the *pkl1Δ* cell, where there is a long MT protrusion (red arrow head), in addition to localizing to the spindle and spindle poles, Cut7-3xGFP also accumulates at the end of the MT protrusion. Scale bar, 5μm.

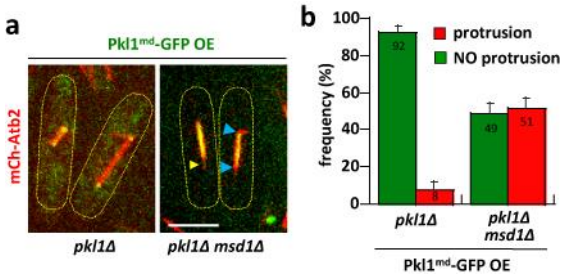

Supplementary Figure 2. Msd1 functions in the same pathway as Pkl1.

a) Images of *pkl1Δ* and double-deletion *pkl1Δ msd1Δ* cells over-expressing (OE) the rigor mutant Pkl1^{md}-GFP. In *pkl1Δ* cells, Pkl1^{md}-GFP can still localize to the spindle poles. In contrast, in *pkl1Δ msd1Δ* cells, Pkl1^{md}-GFP binds along the spindle length, with no clear accumulation at the spindle poles (blue arrow head). Note that MT protrusion (yellow arrow head) can be seen in the *pkl1Δ msd1Δ* cells expressing Pkl1^{md}-GFP. Scale bar, 5μm.

b) Comparative plot of frequency of MT protrusions in *pkl1Δ* (n=38) and *pkl1Δ msd1Δ* (n=39) cells expressing Pkl1^{md}-GFP. The *pkl1Δ* cells have 8% MT protrusion, indicating that the rigor Pkl1^{md}-GFP can mostly (but not completely) rescue the *pkl1Δ* MT protrusion phenotype (see Fig. 2e for comparison). The *pkl1Δ msd1Δ* cells have 51% MT protrusion, indicating that in the absence of Msd1, the rigor Pkl1^{md}-GFP can partially rescue the *msd1Δ* MT protrusion phenotype (see Fig. 2e for comparison). Bars represent mean ± s.d. for multiple experiments.

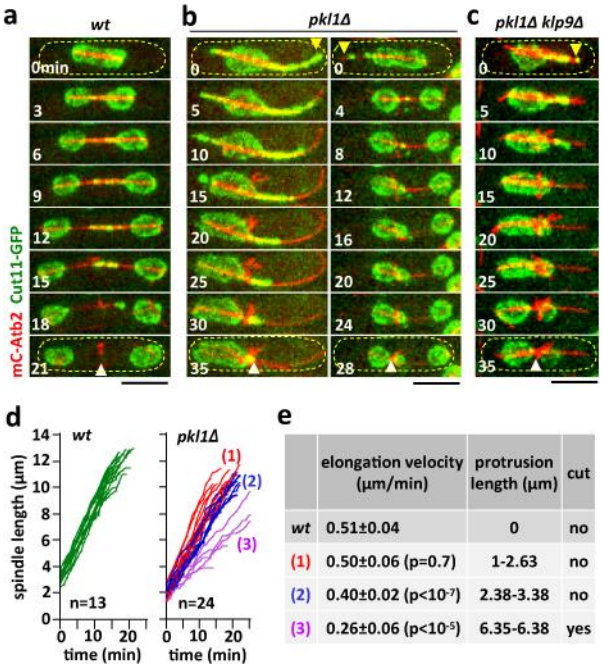

	elongation velocity (μm/min)	protrusion length (μm)	cut
wt	0.51±0.04	0	no
(1)	0.50±0.06 (p=0.7)	1-2.63	no
(2)	0.40±0.02 ($p<10^{-7}$)	2.38-3.38	no
(3)	0.26±0.06 ($p<10^{-5}$)	6.35-6.38	yes

Supplementary Figure 3. Long MT protrusions lead to chromosome cut.

Time-lapse images of *wt*, *pkl1Δ*, and *pkl1Δ klp9Δ* cells expressing mCherry-Atb2 and Cut11-GFP. **a)** The *wt* cell shows symmetric and equal segregation of the daughter nuclei into daughter cells at cytokinesis (white arrow head). **b)** In contrast, *pkl1Δ* cells can have unequal distribution of daughter nuclei. The first panel shows one daughter cell with 2 nuclei and its sister with no nucleus. The second panel shows one daughter cell with 1 nucleus and a micro-nucleus, with its sister having less than 1N chromosome. **c)** The double-deletion *pkl1Δ klp9Δ* cell shows one daughter cell with 1 large nucleus and, with its sister having a small nucleus. Scale bar, 5μm.

d) Spindle length versus time plots comparing anaphase B spindle dynamics of *wt* and *pkl1*Δ cells. In contrast to *wt*, spindle dynamics in *pkl1*Δ cells are varied, approximately falling into three groups. Group (1) has similar dynamics as *wt*. Group (2) has slower elongation dynamics compared to *wt*, but exhibits no chromosome loss. Group (3) is markedly different than *wt*, and has aneuploidy.

e) Quantification of spindle dynamics, protrusion lengths, and aneuploidy in *wt* and *pkl1Δ* cells. Shown are mean ± s.d. Student-t test provides p values.

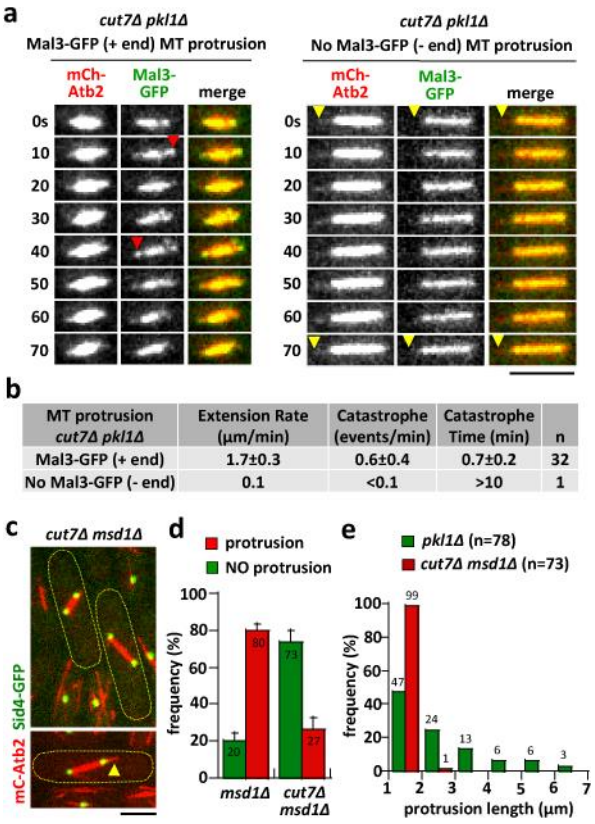

Supplementary Figure 4. Cut7 functions to slide minus-ended MTs into long protrusions.

a) High-temporal resolution (10s interval) time-lapse images of mitotic spindles of *cut7Δ pkl1Δ* cells expressing mCherry-Atb2 and Mal3-GFP. We observed only short MT protrusions (23 mitotic cells, 32 independent MT protrusions). First panel, the short MT protrusion has Mal3-GFP at it end (red arrow head). Second panel, we observed only 1 MT protrusion with no Mal3-GFP at its end (in 23 mitotic cells). Scale bar, 5μm.

b) Comparison of MT dynamic parameters between MT protrusions with and without Mal3-GFP localization at their ends in *cut7Δ pkl1Δ* cells. Based on the relative stability of the one MT end without Mal3-GFP, this end can be classified as minus end.

c) Images of double-deletion *cut7Δ msd1Δ* cells expressing mCherry-Atb2 and Sid4-GFP. The *cut7Δ msd1Δ* cells formed bipolar spindles, and showed only short MT protrusions (yellow arrow head), similar to *cut7Δ pkl1Δ* cells (see Fig. 4b). This indicates that Msd1 and Pkl1 function in the same pathway.

d) Comparative plot of frequency of MT protrusions in *msd1Δ* (n=48) and *cut7Δ msd1Δ* (n=47) cells. The *msd1Δ* cells have 80% MT protrusion. In contrast, *cut7Δ msd1Δ* cells have 27% MT protrusion, indicating that Cut7 functions to slide the unfocused MT minus ends in *msd1Δ* cells producing the aberrant MT protrusions. Bars represent mean ± s.d. for multiple experiments.

e) Plot of MT protrusion length distribution frequency in *pkl1Δ* and *cut7Δ msd1Δ* cells. For *pkl1Δ* cells, MT protrusions extend from 1μm (the defined minimum length for reliable measurement) up to 7μm. 71% of protrusions are shorter than 3μm, and 29% of protrusions are longer than 3μm. In contrast, all MT protrusions are shorter than 3μm in the *cut7Δ msd1Δ* cells. This suggests that Msd1 and Pkl1 are in the same pathway (compare with Fig. 1e and Fig. 4d), and that Cut7 functions to produce minus end MT protrusions in *msd1Δ* (or *pkl1Δ*) cells. Frequencies are pooled from multiple experiments.

Supplementary Table 1. List of Strains

Strain	Genotype
PT.3219	sid4-GFP:KanR mCherry-atb2:HphR ade6-m210 leu1-32 ura4-D18 h-
PT.3280	pkl1Δ:NatR sid4-GFP:KanR mCherry-atb2:HphR ade6-m210? leu1-32 ura4-D18 h+
PT.3207	cut11-GFP:NatR mCherry-atb2:HphR ade6-m210? leu1-32 ura4-D18 h+
PT.3210	pkl1Δ:KanR cut11-GFP:NatR mCherry-atb2:HphR ade6-m210? leu1-32 ura4-D18 h+
CF.658	mini Chromosome ch16:ADE6+ ade6-m216 leu1-32 his2 h+
PT.3774	pkl1Δ:NatR miniChromosome ch16:ade6-m216 leu1-32 his2 h-
PT.3841	pkl1Δ:NatR mal3-linker-GFP:KanR mcherry-atb2:HphR ade6-m210? leu1-32 ura4-D18 h?
PT.2973	cut7-3xGFP:KanMX mCherry-atb2:hph ade6-m210? leu1-32 ura4-D18 h-
PT.3380	pkl1Δ:NatR cut7-3xGFP:KanMX mCherry-atb2:hph ade6-m210? leu1-32 ura4-D18 h+
PT.3765	msd1Δ:KanR sid4-GFP:KanR mCherry-atb2:HphR ade6-m210 leu1-32 ura4-D18 h-
PT.3767	pkl1Δ:NatR msd1Δ:KanR sid4-GFP:KanR mCherry-atb2:HphR ade6-m210 leu1-32 ura4-D18 h-
PT.2753	pkl1-3xGFP:KanR mCherry-atb2:HphR ade6-m210? leu1-32 ura4-D18 h+
PT.3559	msd1Δ:NatR pkl1-3xGFP:KanR mCherry-atb2:HphR ade6-m210 leu1-32 ura4-D18 h+
PT.3477	msd1-GFP:KanR mCherry-atb2:HphR ade6-m210? leu1-32 ura4-D18 h-
PT.3480	pkl1Δ:NatR msd1-GFP:KanR mCherry-atb2:HphR ade6-m210? leu1-32 ura4-D18 h-
PT.3808	nmt-pkl1-GFP:LEU1+ pkl1Δ:KanR mCherry-atb2:HphR ade6-m210? leu1-32 h-
PT.3937	nmt-pkl1-GFP:LEU1+ pkl1Δ:KanR msd1Δ:NatR mCherry-atb2:HphR ade6-m210? leu1-32 ura4-D18 h-
PT.3981	msd1Δ:KanR mCherry-atb2:HphR ade6-m210? leu1-32 ura4-D18 h+ [pPT.419 nmt1-msd1-YFP:URA4+]
PT.3985	msd1Δ:KanR pkl1Δ:NatR mCherry-atb2:HphR ade6-m210? leu1-32 ura4-D18 h- [pPT.419 nmt1-msd1-YFP:URA4+]
PT.3775	msd1Δ:NatR miniChromosome ch16:ade6-m216 leu1-32 his2 h?
PT.3777	pkl1Δ:NatR msd1Δ:KanR miniChromosome ch16:ade6-m216 leu1-32 his2 h?
PT.3811	nmt-rigor-pkl1-GFP:LEU1+ pkl1Δ:KanR mCherry-atb2:HphR ade6-m210? leu1-32 h-
PT.3939	nmt-rigor-pkl1-GFP:LEU1+ pkl1Δ:KanR msd1Δ:NatR mCherry-atb2:HphR ade6-m210? leu1-32 h+
CF.124	mis12-GFP:LEU1+ mCherry-atb2:HphR ade6-m210 leu1-32 ura4-D18 h-
PT.3235	pkl1Δ:KanR mis12-GFP:LEU1+ mCherry-atb2:HphR ade6-m210? leu1-32 ura4-D18 h?
PT.3251	hht2-GFP:URA4+ mCherry-atb2:HphR ade6-m210? leu1-32 ura4-D18 h-
PT.3382	pkl1Δ:NatR hht2-GFP:URA4+ mcherry-atb2:hph ade6-m210? leu1-32 ura4-D18 h+
PT.3681	pkl1Δ:KanR hht2-GFP:URA4+ mcherry-atb2:hph ade6-m210? leu1-32 ura4-D18 h-
PT.3818	pkl1Δ:NatR mad2Δ: KanR mis12-GFP:LEU1+ mCherry-atb2:HphR ade6-m210? leu1-32 ura4-D18 h?
PT.4043	klp9Δ:URA4+ pkl1Δ:KanR cut11-GFP:NatR mCherry-atb2:HphR ade6-m210? leu1-32 ura4-D18 h-
PT.3763	pkl1Δ:NatR klp9Δ:URA4+ sid4-GFP:KanR mCherry-atb2:HphR ade6-m210? leu1-32 ura4-D18 h?
PT.3729	pkl1Δ:KanR cut7Δ:NatR+ sid4-GFP:KanR mCherry-atb2:HphR ade6-m210? leu1-32 ura4-D18 h-
PT.3942	hht2-GFP:URA4+ mCherry-atb2:HphR cdc25-22 ade6-m210? leu1-32 ura4-D18 h-
PT.3944	pkl1Δ:NatR hht2-GFP:URA4+ mCherry-atb2:HphR cdc25-22 ade6-m210? leu1-32 ura4-D18 h-
PT.4003	cut7Δ:NatR pkl1Δ:KanR mal3-linker-GFP:KanR mcherry-atb2:HphR ade6-m210? leu1-32 ura4-D18 h-
PT.4060	msd1Δ:KanR cut7Δ:NatR sid4-GFP:KanR mCherry-atb2:HphR ade6-m210? leu1-32 ura4-D18 h+